

STRUCTURE NOTE

Crystal structures of holo and Cu-deficient Cu/Zn-SOD from the silkworm *Bombyx mori* and the implications in amyotrophic lateral sclerosis

Nan-Nan Zhang, Yong-Xing He, Wei-Fang Li, Yan-Bin Teng, Jiang Yu, Yuxing Chen, and Cong-Zhao Zhou*

Hefei National Laboratory for Physical Sciences at Microscale and School of Life Sciences, University of Science and Technology of China, Hefei 230026, Anhui, People's Republic of China

Key words: protein structure; Cu/Zn superoxide dismutase; amyotrophic; lateral sclerosis; *Bombyx mori*; aggregation; fibril.

INTRODUCTION

Cu/Zn superoxide dismutases (Cu/Zn-SODs) are a large family of cytosolic antioxidant proteins involved in responses to oxidative stress.¹ They catalyze the disproportionation of superoxide radicals into less toxic hydrogen peroxide and dioxygen via cyclic reduction and reoxidation of its bound copper ion as shown below.²



Most of the Cu/Zn-SODs are homodimeric in solution with one copper and one zinc ion per subunit. Each subunit folds as an eight-strand Greek-key β -barrel stabilized by an intrasubunit disulfide bond near the active site.³ Two major structural elements protruding from the β -barrel are termed electrostatic loop and zinc loop. The electrostatic loop connecting $\beta 6$ and $\beta 7$ has positively charged residues finely arranged around the active site to facilitate the diffusion of the negatively charged superoxide anion.⁴ The zinc loop contains two distinct substructures, one of which is anchored to the β -barrel via the disulfide bond between Cys57 and Cys146 and is thus called “disulfide loop.” The other substructure includes all four zinc ligands and forms the zinc binding site. The electrostatic loop and zinc loop are bridged via hydrogen bonds between the nonligand nitrogen of the copper

ligand His46 and the side chain of Asp124. These two structural elements form the substrate accessing channel leading to the active site.³

Mutations in human Cu/Zn-SOD (*hSOD1*) are associated with about 20% of the familial cases of amyotrophic lateral sclerosis (fALS), which is known as one of the neurodegenerative disorders characterized by the progressive loss of motor neurons in brains and spinal cord leading to paralysis and eventual death.^{5,6} The mutations in fALS-linked *hSOD1* (fALS-*hSOD1*) have been mapped to nearly all regions, including the dimeric interface, loop regions, β -barrel, disulfide bond cysteines, and the Cu/Zn ligands (a full list can be found at <http://www.alsod.org>). It was first believed that the fALS-*hSOD1* had impaired enzymatic activity leading to the increased oxidative damage to neurons.⁷ However, with the identification of more fALS associated human SOD1 mutants,

Grant sponsor: Chinese National Natural Science Foundation; Grant number: 90608027; Grant sponsor: Hi-Tech Research and Development Program of China; Grant number: 2006AA10A119; Grant sponsor: The 973 project from the Ministry of Science and Technology of China; Grant numbers: 2005CB121002 and 2006CB910202; Grant sponsor: Knowledge Innovation Program from Chinese Academy of Science.

*Correspondence to: Cong-Zhao Zhou, Hefei National Laboratory for Physical Sciences at Microscale and School of Life Sciences, University of Science and Technology of China, Hefei 230026, Anhui, People's Republic of China.

E-mail: zcz@ustc.edu.cn

Received 11 January 2010; Accepted 11 February 2010

Published online 1 March 2010 in Wiley InterScience (www.interscience.wiley.com). DOI: 10.1002/prot.22709

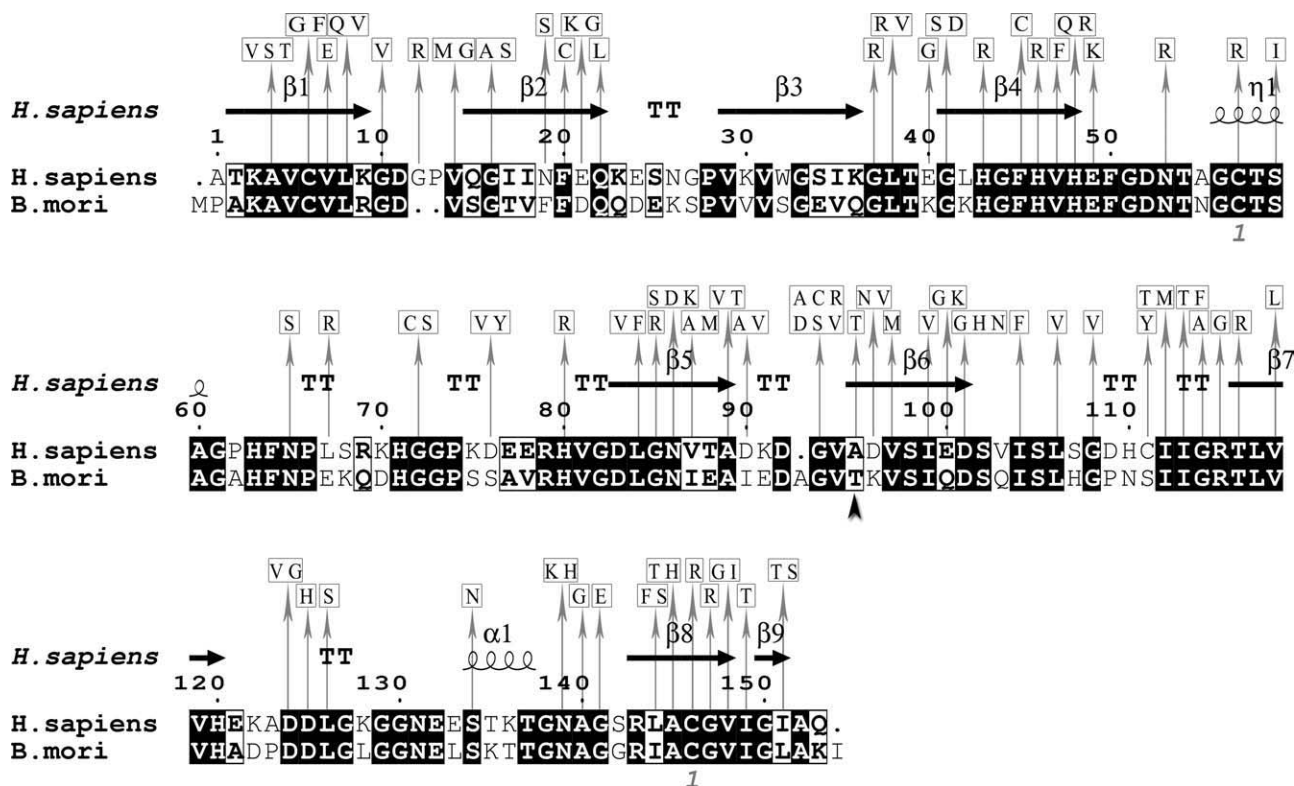


Figure 1

Pairwise alignment of *BmSod1* and *hSOD1*. The alignment was performed using MultAlin¹⁸ and ESPrpt.¹⁹ The secondary structural elements of *hSOD1* are displayed at the top of the alignment. The α -helices, β -strands, β -sheets, and strict β -turns are denoted α , η , β , and TT, correspondingly. The mutation sites related to ALS were annotated and T96 of *BmSod1* was marked by a filled circle.

the majority of these mutant proteins were biochemically characterized to have enzymatic activity comparable to the wild-type, suggesting that these mutations are most likely to confer a dominant toxicity on the protein, rather than a loss-of-function.^{8,9} This hypothesis is strongly supported by the mouse model of ALS disease in which the transgenic mice expressing fALS associated mutants of *hSOD1* develop a late-onset progressive motor neuron disease that mimics the human disease,¹⁰ in contrast with the *SOD1* knock-out mice that do not show any of the ALS symptoms.¹¹ Although the mechanism of the toxicity is still unknown, the aberrant aggregation of *SOD1* mutant proteins is strongly suggested to play important roles in the etiology of the disease.¹² Several fALS associated *hSOD1* mutant proteins have been confirmed *in vitro* to form soluble oligomers or even linear/helical fibrils via nonnative interfaces.^{13–16}

The Cu/Zn-SOD from the silkworm *Bombyx mori* (*BmSod1*) shares 63% sequence identity with *hSOD1*, with 56 different residues out of the total 153 residues and a number of these “substituted” sites can be mapped to the ALS-linked *hSOD1* mutation sites (Fig. 1). Here, we report the crystal structures of *BmSod1* in both holo and Cu-deficient forms. Structural analyses reveal that

both forms are arranged as helical fibrils and further into water-filled nanotubes via nonnative interfaces in the crystalline environment. Combined with sequence analysis, it was suggested that amino acid substitution in those regions responsible for forming nonnative interfaces may impair the *hSOD1*-like native conformation, which originally opposes aggregation by negative design.¹⁷

MATERIALS AND METHOD

Cloning, expression and purification of *BmSod1*

Total RNA was extracted from the silkglands of 5th instar larvae of the silkworm P50 with Trizol reagent. The first strand of cDNA was synthesized from 20 ng of the total RNA using Super Script II reverse transcriptase and random primer. The target gene was then amplified using sense (5'CGTCTCATATGCCCGCCAAAGCAGTT3') and antisense (5'CTTGCGCCGCTTAAATCTTGCCAA GCC3') primers. The amplified fragments encoding *BmSod1* were then cloned to a modified pET28a vector (Novagen) with an additional 6 \times His coding sequence at the 5' end of the genes. The recombinant plasmid was

transformed into *E. coli* Rosetta (DE3) competent cells, which were cultured in 400 mL 2×YT with supplement of 0.01 mg/ml kanamycin. The culture was grown at 37°C to an $A_{600\text{ nm}}$ of 0.6 and induced with 0.2 mM IPTG for 4 h. After harvesting, cells were resuspended in 50 mL buffer of 100 mM NaCl, 20 mM Tris-HCl, pH 8.0. After three cycles of freeze-thaw followed by 3 min sonication, the lysed cells were centrifuged at 16,000g for 20 min. The supernatant was loaded onto either a Ni²⁺-NTA or a Cu²⁺-NTA affinity column (GE Healthcare) followed by gel filtration using Superdex 75 column (Amersham Biosciences) equilibrated with 100 mM NaCl, 20 mM Tris-HCl, pH 8.0, 14 mM β-mercaptoethanol. The purity of the fractions was checked on the SDS-PAGE.

Crystallization and data collection

The protein sample was crystallized using the hanging-drop vapor-diffusion method at 289 K. *BmSod1* purified with Ni²⁺-NTA column is Cu-deficient and the crystals of Cu-deficient *BmSod1* were grown from a mixture of equal volumes of 20 mg/ml protein in 100 mM NaCl, 20 mM Tris-HCl pH 8.0, 14 mM β-mercaptoethanol, 10 mM DTT and a 400 mL reservoir solution consisting of 0.2M calcium acetate, 0.1M sodium cacodylate pH 6.5, 17% PEG 4K, 15% isopropanol. When purified with Cu²⁺-NTA, the copper content of *BmSod1* can be restored and the crystals of holo *BmSod1* were grown from a mixture of equal volumes of 10 mg/ml protein in 100 mM NaCl, 20 mM Tris-HCl pH 8.0, and a 400 μl reservoir solution consisting of 2.0 M (NH₄)₂SO₄, 0.1M Tris-HCl, pH 8.5, 10% glycerol, 1 mM CuCl₂. Diffraction data of Cu-deficient *BmSod1* were collected in a stream of nitrogen gas at 100K using a Rigaku MM007 X-ray generator ($\lambda = 1.54178 \text{ \AA}$) with a MarResearch 345 image-plate detector at School of Life Sciences, University of Science and Technology of China (USTC, Hefei, China). The data were processed with the program MOSFLM 7.0.4²⁰ and scaled with SCALA.²¹ Diffraction data of holo *BmSod1* were collected at a wavelength of 0.9794 Å at Shanghai Synchrotron Radiation Facility (SSRF) using beamline 17U at 100 K with a MX225 CCD (MARresearch, Germany). The diffraction data was indexed, integrated, and scaled with HKL2000.²²

Structure determination and refinement

The structure of Cu-deficient *BmSod1* was solved by the molecular replacement method with the program *MOLREP*²³ using the wild-type *hSOD1* (PDB code 1AZV) as the search model. Two dimers were located in the crystallographic asymmetric unit. The initial model was refined by using the maximum likelihood method implemented in *REFMAC5*²⁴ as part of *CCP4*²⁵ program suite and rebuilt interactively by using the σ_A -weighted

electron density maps with coefficients 2mFo-DFc and mFo-DFc in the program *COOT*.²⁶ Five percent of reflections were set aside to calculate an R-free factor. Each monomer was refined independently, without application of noncrystallographic symmetry restraints. Bulk solvent correction was applied and solvent molecules were added using *COOT*. Refinement finally converged to a R-factor of 20.1% and R-free of 24.8% at a resolution of 2.05 Å.

The holo *BmSod1* structure was also determined by the molecular replacement method with *MOLREP* using the coordinates of a monomer of the Cu-deficient *BmSod1* as the search model. One dimer was located in the asymmetric unit. The initial model was refined using the program *REFMAC5* and manually rebuilt in the program *COOT*. No NCS restraints were applied during the refinement. Refinement finally converged to a R-factor of 22.3 and R-free of 25.8% at a resolution of 1.80 Å. To reduce geometry bias of the metal ligands, no stereo-chemical restraints on metal ligand bonds or angles were applied. Both models were validated by using the program *MOLPROBITY*²⁷ to correct the obvious clashes and bad rotamers in the later stages of refinement. The final models were evaluated with the programs *MOLPROBITY* and *PROCHECK*.²⁸ The final coordinates and structure factors were deposited in the Protein Data Bank (<http://www.rcsb.org/pdb>) under the accession codes of 3L9E and 3L9Y for Cu-deficient and holo *BmSod1*, respectively. The data collection and structure refinement statistics were listed in Table I. The buried surface area was calculated with *AREAIMOL* as part of the CCP4i program suite and the solvation free energy gain $\Delta^{\ddagger}G$ was calculated with the EMBL-EBI *PISA* server²⁹ (http://www.ebi.ac.uk/msd-srv/prot_int/cgi-bin/piserver). All structure figures were prepared with the program *PyMOL*.³⁰

RESULTS

Overall structures and active sites

The recombinant *BmSod1* produced by *E. coli* has extremely low occupancy of copper, as indicated by atomic absorption spectroscopy, and we thus refer to it as Cu-deficient *BmSod*. We restored the copper content by chromatography in a Cu-NTA column, and refer to that protein as holo *BmSod*. The crystal of Cu-deficient *BmSod1* crystal diffracts to 2.05 Å resolution and belongs to the *P*6₅ space group, with four molecules in an asymmetric unit, whereas that of holo *BmSod1* diffracts to 1.80 Å resolution and belongs to the *P*6₄ space group, with two molecules in an asymmetric unit.

The overall structures of the holo as well as the Cu-deficient *BmSod1* preserve the typical Cu/ZnSOD tertiary structure, which adopts a flattened Greek-key β-barrel motif consisting of eight antiparallel β-strands connected by loops, turns or short α-helices [Fig. 2(A)]. The copper binding site of Cu-deficient *BmSod1* was not perturbed

Table 1
Crystal Parameters, Data Collection and Structure Refinement

	Holo BmSOD1	Cu-deficient BmSOD1
Data processing		
Space group	$P6_4$	$P6_5$
Unit cell parameters a, b, c (Å)	111.49, 111.49, 39.89	118.47, 118.47, 81.79
α, β, γ (°)	90, 90, 120	90, 90, 120
Resolution range (Å)	30.00–1.80 (1.86–1.80) ^a	23.99–2.04 (2.15–2.04)
Unique reflections	26262 (2560)	41012 (5335)
Completeness (%)	99.4 (99.0)	97.8 (87.0)
$\langle I/\sigma(I) \rangle$	21.3 (5.2)	11.0 (2.8)
R_{merge}^b (%)	7.0 (29.7)	10.3 (47.0)
Redundancy	7.1 (6.2)	3.9 (3.5)
Refinement statistics		
Resolution range (Å)	30.00–1.80	23.00–2.05
R-factor ^c /R-free ^d (%)	22.3/25.8	20.1/24.8
Number of protein atoms	2367	4448
Number of metal ions	4	4
Number of water atoms	153	483
RMSD ^e bond length (Å)	0.006	0.007
RMSD bond angles (°)	1.004	1.072
Average of B factors (Å ²)	28.5	20.68
Ramachandran plot ^f		
Most favored (%)	99.0	98.03
Additional allowed (%)	1.0	1.97
Outliers (%)	0	0
PDB entry	3L9Y	3L9E

^aThe values in parentheses refer to statistics in the highest bin.

^b $R_{\text{merge}} = \sum_{\text{hkl}} \sum_i |I_i(\text{hkl}) - \langle I(\text{hkl}) \rangle| / \sum_{\text{hkl}} \sum_i I_i(\text{hkl})$, where $I_i(\text{hkl})$ is the intensity of an observation and $\langle I(\text{hkl}) \rangle$ is the mean value for its unique reflection; Summations are over all reflections.

^cR-factor = $\sum_h |F_o(h) - F_c(h)| / \sum_h F_o(h)$, where F_o and F_c are the observed and calculated structure-factor amplitudes, respectively.

^dR-free was calculated with 5% of the data excluded from the refinement.

^eRoot-mean square-deviation from ideal values.

^fCategories were defined by Molprobability.

by copper deletion and structures of both holo and Cu-deficient *BmSod1* dimers are quite similar, with an overall root mean square deviation (RMSD) of 0.4 Å over 289 C α atoms (Fig. 2B, 2C). Two monomers assemble into a tight dimer through mutual interactions between loop IV and strand β 8, with a buried surface area of ~ 750 Å². The two strictly conserved residues Cys56 and Cys146 form an intrasubunit disulfide bond that anchors loop IV to the β -barrel scaffold. These two cysteines are essential for the enzyme's folding. All these structural features are very similar to those of *hSOD1* as well as Cu/Zn SODs from other species.

Helical fibril of *BmSod1* due to crystal packing

ALS-linked *hSOD1* mutants, such as S134N, H46R, and Zn-H46R (zinc bound H46R mutant), have been reported to form either linear or helical filaments in the crystalline environment via newly gained “nonnative” interfaces. The electrostatic loop or zinc loop in these mutant proteins is partially disordered and adopts a nonnative conformation that packs onto edges of strands β 5 and β 6.¹⁴ Strikingly, crystal packing of both holo and Cu-deficient *BmSod1* showed helical fibril arrangement quite similar to the Zn-

H46R mutant of *hSOD1*. In the case of *hSOD1* Zn-H46R, zinc loop residues 78–81 adopt a nonnative conformation and hydrogen bond to the deprotected beta-edge of the β 6, resulting in a nonnative interface of 550 Å². Repetition of this nonnative interface yields hollow nanotubes with an overall diameter of 95 Å and an inner diameter of 30 Å. For the two structures of *BmSod1*, the newly emerged nonnative interface is also formed by the zinc loop (involving residues P73, S74, S75, and A76) from one dimer packing onto the exposed edge of strand S6 (involving S98, I99, Q100, and S102) from the neighboring subunit, leading to helical fibrils with a diameter of ~ 120 Å and a translation of ~ 190 Å per turn (i.e., six dimers). The buried interface is up to ~ 650 Å², with a solvation free energy gain ($\Delta^i G$) of -5.3 kcal/mol, which is comparable to the typical tight dimeric interface of ~ 750 Å², with a $\Delta^i G$ of -8.9 kcal/mol [Fig. 2(D)]. The helical fibrils further stick together to form a water-filled nanotube with an outer diameter of ~ 120 Å and a water-filled inner cavity of ~ 40 Å in diameter (Fig. 2E, 2F). The interface between helical fibrils buried up to ~ 450 Å² ($\Delta^i G$ -4.2 kcal/mol) on average [Fig. 2(D)], involving interactions between the electrostatic loop residues E132-L133 and zinc loop residues E66-K67.

The fibril arrangement of holo and Cu-deficient *BmSod1* in the crystalline environment suggests an ALS-

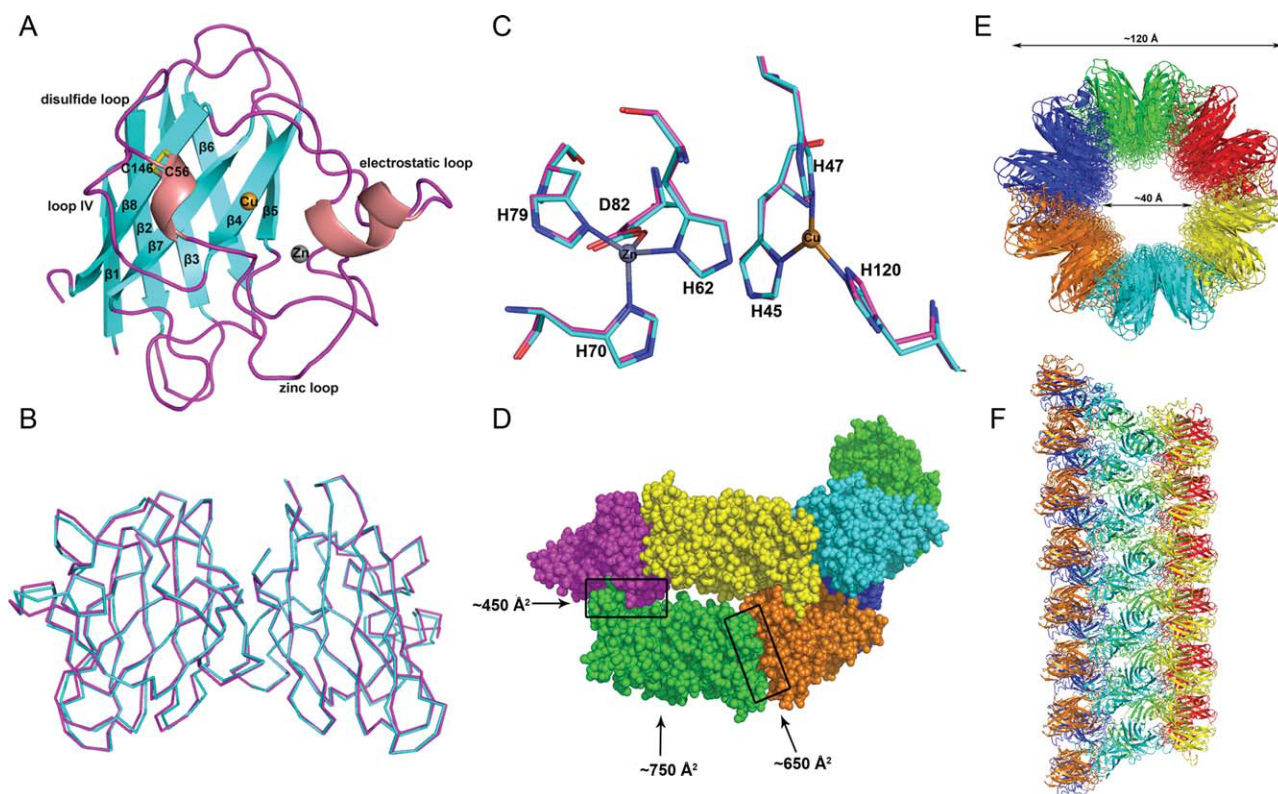


Figure 2

A: Cartoon representation of the holo *BmSod1* monomer. The bound zinc and copper ions were shown in sphere. **B:** Superposition of the dimers of holo (cyan) and Cu-deficient *BmSod1* (pink). **C:** Superposition of the zinc and copper binding sites of holo (cyan) and Cu-deficient *BmSod1* (pink). **D:** Fibril assembly interfaces of *BmSod1*, the nonnative interfaces were boxed with black rectangles. **E** and **F:** Top view and front view of the water-filled nanotube of *BmSod1*.

linked mutant-like nature of the wild-type *BmSod1*. The nonnative interface involved in fibril assembly is located in the electrostatic loop, zinc loop, and strand $\beta 6$, all of which are suggested as major candidates for forming aggregation-prone interfaces.¹⁴ For ALS-linked *hSOD1* mutants, structural perturbation because of metal depletion is proved to be responsible for the emergence of nonnative interfaces.^{14,31} However, for either holo or Cu-deficient *BmSod1*, both the zinc loop and electrostatic loop remain intact, prompting us to speculate that the amino acid substitution in those regions may impair the *hSOD1*-like native conformation which originally opposes aggregation by negative design. Indeed, the “SSAV” tetrad (residues 74–77) from the zinc loop of *BmSod1* accounting for the helical fibril assembly were replaced by a tetrad of ionizable amino acid “KDEE” in *hSOD1* (Fig. 1), which may prevent the nonnative contacts through electrostatic and/or steric repulsion of the bulky charged side-chains. Also, the residues participating in the fibril-fibril stacking of *BmSod1*, such as E66, K67, and L133, are replaced by different types of residues in *hSOD1* so that nonnative contacts could possibly be avoided.

Being aggregation prone as *hSOD1* mutants, why the wild-type *BmSod1* does not have apparent toxic effects on *Bombyx mori* neurons and cause ALS-like symptoms? One possible reason is that ALS is a progressive and long term disease. Unlike humans, the life span of *Bombyx mori* may not be long enough for the wild-type *BmSod1* to form insoluble aggregates or cause the loss of the motor neurons. It has been reported that the exogenously expressed wild-type *hSOD1* as well ALS mutants in *Drosophila* motor neurons did not form high molecular weight aggregates from 1–49 days.³² Collectively, we speculate that Cu/Zn-SOD might be an intrinsically aggregation-prone protein during earlier stages of phylogenesis, but undergo substantial site mutations opposing self-aggregation during evolution because endogenous protein aggregates are highly toxic and even lethal to mammalian/human neurons.

REFERENCES

1. Mccord JM, Fridovich I. The utility of superoxide dismutase in studying free radical reactions. I. Radicals generated by the interaction of sulfite, dimethyl sulfoxide, and oxygen. *J Biol Chem* 1969;244:6056–6063.

2. Fridovich I. Superoxide dismutases. *Annu Rev Biochem* 1975;44: 147–159.
3. Tainer JA, Getzoff ED, Beem KM, Richardson JS, Richardson DC. Determination and analysis of the 2 A-structure of copper, zinc superoxide dismutase. *J Mol Biol* 1982;160:181–217.
4. Stroppolo ME, Falconi M, Caccuri AM, Desideri A. Superefficient enzymes. *Cell Mol Life Sci* 2001;58:1451–1460.
5. Brown RH. Superoxide dismutase in familial amyotrophic lateral sclerosis: models for gain of function. *Curr Opin Neurobiol* 1995;5: 841–846.
6. Brown RH. Amyotrophic lateral sclerosis: recent insights from genetics and transgenic mice. *Cell* 1995;80:687–692.
7. Deng HX, Hentati A, Tainer JA, Iqbal Z, Cayabyab A, Hung WY, Getzoff ED, Hu P, Herzfeldt B, Roos RP, Warner C, Deng G, Soriano E, Smyth C, Parge HE, Ahmed A, Roses AD, Hallewell RA, Pericak-Vance MA, Siddique T. Amyotrophic lateral sclerosis and structural defects in Cu,Zn superoxide dismutase. *Science* 1993;261:1047–1051.
8. Borchelt DR, Guarnieri M, Wong PC, Lee MK, Slunt HS, Xu ZS, Sisodia SS, Price DL, Cleveland DW. Superoxide dismutase 1 subunits with mutations linked to familial amyotrophic lateral sclerosis do not affect wild-type subunit function. *J Biol Chem* 1995;270: 3234–3238.
9. Rabizadeh S, Gralla EB, Borchelt DR, Gwinn R, Valentine JS, Sisodia S, Wong P, Lee M, Hahn H, Bredesen DE. Mutations associated with amyotrophic lateral sclerosis convert superoxide dismutase from an antiapoptotic gene to a proapoptotic gene: studies in yeast and neural cells. *Proc Natl Acad Sci USA* 1995;92:3024–3028.
10. Tu PH, Raju P, Robinson KA, Gurney ME, Trojanowski JQ, Lee VM. Transgenic mice carrying a human mutant superoxide dismutase transgene develop neuronal cytoskeletal pathology resembling human amyotrophic lateral sclerosis lesions. *Proc Natl Acad Sci USA* 1996;93:3155–3160.
11. Reaume AG, Elliott JL, Hoffman EK, Kowall NW, Ferrante RJ, Siwek DF, Wilcox HM, Flood DG, Beal MF, Brown RH, Scott RW, Snider WD. Motor neurons in Cu/Zn superoxide dismutase-deficient mice develop normally but exhibit enhanced cell death after axonal injury. *Nat Genet* 1996;13:43–47.
12. Furukawa Y, Fu R, Deng HX, Siddique T, O'halloran TV. Disulfide cross-linked protein represents a significant fraction of ALS-associated Cu, Zn-superoxide dismutase aggregates in spinal cords of model mice. *Proc Natl Acad Sci USA* 2006;103:7148–7153.
13. Hart PJ. Pathogenic superoxide dismutase structure, folding, aggregation and turnover. *Curr Opin Chem Biol* 2006;10:131–138.
14. Elam JS, Taylor AB, Strange R, Antonyuk S, Doucette PA, Rodriguez JA, Hasnain SS, Hayward LJ, Valentine JS, Yeates TO, Hart PJ. Amyloid-like filaments and water-filled nanotubes formed by SOD1 mutant proteins linked to familial ALS. *Nat Struct Biol* 2003;10:461–467.
15. Antonyuk S, Elam JS, Hough MA, Strange RW, Doucette PA, Rodriguez JA, Hayward LJ, Valentine JS, Hart PJ, Hasnain SS. Structural consequences of the familial amyotrophic lateral sclerosis SOD1 mutant His46Arg. *Protein Sci* 2005;14:1201–1213.
16. Didonato M, Craig L, Huff ME, Thayer MM, Cardoso RM, Kassmann CJ, Lo TP, Bruns CK, Powers ET, Kelly JW, Getzoff ED, Tainer JA. ALS mutants of human superoxide dismutase form fibrous aggregates via framework destabilization. *J Mol Biol* 2003; 332:601–615.
17. Richardson JS, Richardson DC. Natural beta-sheet proteins use negative design to avoid edge-to-edge aggregation. *Proc Natl Acad Sci USA* 2002;99:2754–2759.
18. Corpet F. Multiple sequence alignment with hierarchical clustering. *Nucl Acids Res* 1988;16:10881–10890.
19. Gouet P, Robert X, Courcelle E. ESPript/ENDscript: Extracting and rendering sequence and 3D information from atomic structures of proteins. *Nucl Acids Res* 2003;31:3320–3323.
20. Leslie AGW. Recent changes to the MOSFLM package for processing film and image plate data. *Joint CCP4 1 ESF-EAMCB Newsletter on Protein Crystallography* 1992;26.
21. Evans PR. Data reduction, In: *Proceedings of CCP4 Study Weekend, on Data Collection and Processing*, Warrington: Daresbury Laboratory; 1993, pp 114–122.
22. Otwinowski Z, Minor W. Processing of X-ray diffraction data collected in oscillation mode. *Macromol Crystallogr* 1997;276:307–326.
23. Vagin A, Teplyakov A. MOLREP: an automated program for molecular replacement. *J Appl Crystallogr* 1997;30:1022–1025.
24. Murshudov GN, Vagin AA, Dodson EJ. Refinement of macromolecular structures by the maximum-likelihood method. *Acta Crystallogr* 1997;53(Part 3):240–255.
25. Leslie, AGW. The CCP4 suite: programs for protein crystallography. *Acta Crystallogr* 1994;50:760–763.
26. Emsley P, Cowtan K. Coot: model-building tools for molecular graphics. *Acta Crystallogr* 2004;60:2126–2132.
27. Davis IW, Leaver-Fay A, Chen VB, Block JN, Kapral GJ, Wang X, Murray LW, Arendall WB, Snoeyink J, Richardson JS, Richardson DC. MolProbity: all-atom contacts and structure validation for proteins and nucleic acids. *Nucl Acids Res* 2007;35:W375–W383.
28. Laskowski RA, MacArthur MW, Moss DS, Thornton JM. Procheck - a Program to Check the Stereochemical Quality of Protein Structures. *J Appl Crystallogr* 1993;26:283–291.
29. Krissinel E, Henrick K. Inference of macromolecular assemblies from crystalline state. *J Mol Biol* 2007;372:774–797.
30. Delano WL. The PyMOL Molecular Graphics System, San Carlos, CA: DeLano Scientific LLC.
31. Cao X, Antonyuk SV, Seetharaman SV, Whitson LJ, Taylor AB, Holloway SP, Strange RW, Doucette PA, Valentine JS, Tiwari A, Hayward LJ, Padua S, Cohlberg JA, Hasnain SS, Hart PJ. Structures of the G85R variant of SOD1 in familial amyotrophic lateral sclerosis. *J Biol Chem* 2008;283:16169–16177.
32. Watson MR, Lagow RD, Xu K, Zhang B, Bonini NM. A drosophila model for amyotrophic lateral sclerosis reveals motor neuron damage by human SOD1. *J Biol Chem* 2008;283:24972–24981.